Geophys. J. Int. (1998) **135,** 691–699

Observations and origin of Rayleigh-wave amplitude anomalies

S. van der Lee*

Department of Terrestrial Magnetism, Carnegie Institution of Washington, Washington, DC 20015, *USA*

Accepted 1998 July 9. Received 1998 July 8; in original form 1998 February 25

SUMMARY

This is a report of observations of amplitude anomalies of fundamental-mode Rayleigh waves (*R*1) between periods of 17 and 100 s. The anomalies are with respect to amplitudes predicted by Rayleigh-wave excitation for a reference earth model and catalogued centroid earthquake source parameters, such as are used in large-scale waveform inversions. The observations indicate that the amplitude anomalies are consistent for nearby recordings of the same event, while there is no obvious relation between the observed anomalies and the paths travelled by the waves. This is in contrast to Rayleigh-wave phase anomalies, which are consistent for similar propagation paths, and hence form the input in many inversions for along-path structure. The observations in this paper show that a similar inversion of intermediate-period amplitude anomalies for along- and near-path structure is not warranted without eliminating source effects, since the amplitude anomalies are dominated by scattering off near-source earth structure and by possible uncertainties in the source parameters. Sensitivity kernels that take the coupling between the moment tensor and displacement field into account demonstrate that Rayleigh-wave amplitude sensitivity is largest near the source. This report argues that the interaction between source-radiated Rayleigh waves and near-source earth structure may not be ignored in amplitude inversion procedures.

Key words: amplitude anomalies, near field, Northridge, propagation corridors, Rayleigh waves, source mechanism.

INTRODUCTION

Amplitudes and phases of teleseismic and regional Rayleigh waves have been successfully used in inversions for source parameters for decades. Amplitude anomalies, between observed and predicted Rayleigh waves, that remain after taking the source parameters into account can be related to

(1) uncertainties or unmodelled details in the source mechanism, depth and average near-source structure;
(2) scattering (multipathing, focusing, defocusing) near the source, along and near the path of wave propagation and near the receiver;
(3) anomalous *Q* (anelastic structure) along the propagation path;
(4) uncertainties in the station site and instrument response to ground displacement.

Phase anomalies that remain after taking the source parameters into account are consistent within propagation corridors and have been successfully explained by anomalous velocity structure (elastic structure) along the propagation path, for example in waveform-fitting tomography for 3-D Earth structure (Woodhouse & Dziewonski 1984; Nolet 1990; Zhang & Tanimoto 1993; Zielhuis & Nolet 1994; Zielhuis & Van der Hilst 1996; Van der Lee & Nolet 1997b). This type of waveform tomography is part of a variety of surface-wave tomography, in which classically it has been assumed that the observed Rayleigh wave travelled straight from the earthquake source along a great-circle ray of infinitesimal width to the seismic station. In reality the observed Rayleigh-wave energy has been distributed, in an unknown way, over the Fresnel zone. The sum of Rayleigh-wave energy that propagated in the Fresnel zone but off the great circle can greatly affect the recorded amplitude. Several methods have been developed and applied to include the effects of off-great-circle propagation (Snieder 1988b; Laske & Masters 1996; Meier *et al.* 1997). Moreover, amplitude anomalies of surface waves have been used as additional constraints on anomalous upper-mantle structure along and near the paths of wave propagation, to shorter and shorter periods, from e.g. 80–320 s (Romanowicz 1995) and 57–400 s (Laske & Masters 1996) to 40–150 s (Alsina, Woodward & Snieder 1996). Woodhouse & Wong (1986)

*Now at: Institut für Geophysik, ETH Hönggerberg (HPP), 8093 Zürich, Switzerland.

© 1998 RAS

developed a linear relationship between small surface-wave amplitude anomalies and the path-averaged curvature in the phase velocity field across the path, and Snieder (1988a) developed a linear relationship between residual waveforms of surface waves and model perturbations near the path. The development of these linear relationships has made the inversion of surface-wave amplitude anomalies for along- and near-path structure feasible and it is tempting to extend such inversion to higher and higher frequencies without testing the contribution of the other factors, listed above, to the observed amplitude anomalies. This paper reports the results of systematic analysis of observed amplitude anomalies of fundamental-mode Rayleigh waves between 17 and 100 s. This analysis leads to the identification of the dominant factors that determine the amplitude anomalies in this intermediate-frequency range.

DATA SELECTION

To study the amplitude anomaly pattern of the fundamental-mode Rayleigh wave, records of Rayleigh waves that travelled practically along the same wave path in a narrow propagation corridor were selected. If the observed amplitude anomalies of these Rayleigh waves are caused by Earth structure along the wave path, such as anomalous Q or scatterers (possibly in the form of curvature in the velocity field), the records should show very similar amplitude anomalies. If the amplitude anomalies are caused by uncertainties in the site or instrument response or by near-receiver scattering, the records should show amplitude anomalies that vary from station to station. If the amplitude anomalies are caused by uncertainties in the source parameters, average near-source structure or near-source scattering, the records should show amplitude anomalies that vary from event to event.

Two clusters of Mexican events were selected that were recorded at closely spaced stations in the United States and Canada, at some 30° epicentral distance. The great-circle paths followed by the waves within each propagation corridor are shown in Fig. 1. An additional, extremely narrow, propagation corridor (Fig. 1) contains the great-circle wave paths from the 1994 Northridge event near Los Angeles and its aftershocks to GSN station HRV. The events are listed in Table 1, and

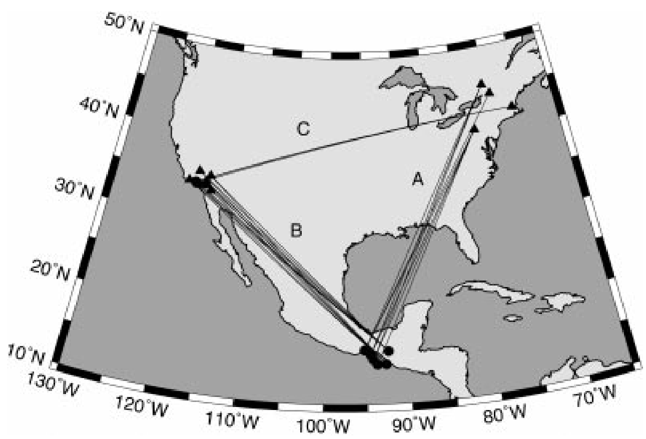

Figure 1. Map showing the propagation corridors of Rayleigh-wave propagation from clusters of events to groups of nearby stations.

Table 2 lists the Harvard centroid source parameters used in this study.

To estimate the similarity of the wave paths within each propagation corridor, the area of overlap $O_{\cup}$ between Fresnel zones for two paths within one corridor can be evaluated. Using eq. (2.7) from Wang & Dahlen (1995) and defining the similarity $\sigma = O_{\cup}/O$, where O is the total area of the Fresnel zone, we find that for any two great-circle ray paths within each propagation corridor, their similarity $\sigma > 80$ per cent at 100 s, $\sigma > 60$ per cent at 30 s and $\sigma > 45$ per cent at 17 s (Van der Lee 1996). The width of the propagation corridors (200 km) is smaller than the average width (330 km) of the smallest Fresnel zone at 17 s. The average width of the Fresnel zone at 100 s is 900 km, while the maximum widths are 420 and 1170 km for 17 and 100 s, respectively. The wave paths are thus sufficiently close for one to expect similar propagation effects from smooth near-path structure in the Rayleigh waves. Waveform fitting of each of the fundamental-mode Rayleigh waves within each propagation corridor by perturbing the path-averaged velocity structure (Nolet 1990) indeed provides very similar velocity models for paths within the same corridor, except for the paths in corridor A from event 830124, which will be discussed separately. The optimal waveform fits are generally dominated by a good match of the observed and synthetic phases of the waves. The remaining waveform misfits mainly consist of a frequency-dependent amplitude anomaly.

PROPAGATION CORRIDOR A

For propagation corridor A (Fig. 1) the observed and synthetic waveforms and their amplitude spectra are shown in Fig. 2. Fig. 2 shows that the relative amplitude anomalies of the Rayleigh waves are *not* similar for the close paths within the corridor. This indicates that the amplitude anomalies cannot be directly related to effects from smoothly varying Earth structure along and across the paths within the corridor. However, it can be seen in Fig. 2 that a significant correlation exists between relative amplitude anomaly spectra of Rayleigh waves from the same event recorded by different stations. This indicates that the relative amplitude anomalies of these fundamental-mode Rayleigh waves are dominated by unmodelled contributions from the earthquake source.

Catalogued source parameters are determined with sophisticated methods and based on as wide a range of data as possible, including body and surface waves in various frequency bands and with good azimuthal coverage (Dziewonski, Chou & Woodhouse 1981; Dziewonski, Ekström & Salganik 1992; Sipkin 1986). Moreover, the centroid source parameters as determined by different agencies generally agree well (Helffrich 1997). It is unlikely that these source parameters can be further optimized to fit in detail the remaining amplitudes anomalies, although uncertainties in some of the source parameters or in the structure of the reference earth model can explain part of these anomalies (Van der Lee 1996; Patton 1998). For example, an adjustment of M_0 can explain most of the anomaly of 870312. A correction in the reported centroid depth of 10 km for 810817 can explain part of the anomaly for this event. For 841013 a deeper hypocentre or a Moho in the source region that is shallower than the standard 35 km reduces the amplitude anomaly for this event. Errors in the reported estimated half-duration can play a role in the larger events, such as 830124. Events 810817, 841013, 870312 and 870315 have a

Table 1. Events used in this study.

Event ID	Propagation corridor	Origin time, UT	Latitude	Longitude	m_b	M_s
810817	A	02:18:58.8	14.52	−93.77	5.5	5.5
830124	A	08:17:39.6	16.15	−95.23	6.3	6.6
841013	A	17:18:14.2	15.06	−94.24	6.1	5.7
870312	A	12:18:11.9	15.72	−94.50	5.7	5.6
870315	A	05:11:17.3	15.67	−94.52	5.6	5.6
930903	B	12:35:0.2	14.52	−93.71	5.8	6.8
940314	B	20:51:24.9	15.99	−92.43	5.9	6.2
940117	C	12:30:55.3	34.21	−118.54	6.4	6.8
940118	C	−26:29.4	34.33	−118.70	5.6	6.0
940119	C	21:09:28.6	34.38	−118.71	5.0	
940320	C	21:20:12.2	34.23	−118.48	5.1	4.8

Table 2. Harvard centroid source parameters of events used in this study.

Event ID	Centroid depth (km)	Duration (s)	Scale of M (Nm)	M_{rr}	$M_{\theta\theta}$	$M_{\phi\phi}$	$M_{r\theta}$	$M_{r\phi}$	$M_{\theta\phi}$
810817	10	6.0	10^{17}	−6.48	4.02	2.46	−9.88	5.67	−3.39
830124	36	18.0	10^{19}	−1.09	0.16	0.93	−0.87	−0.93	−1.29
841013	16	7.4	10^{17}	6.28	−4.60	−1.69	4.95	−5.06	2.41
870312	17	7.6	10^{18}	0.80	−1.01	0.21	1.20	−0.04	0.12
870315	40	6.6	10^{17}	4.77	−3.30	−1.47	3.47	−3.81	3.48
930903	27	11.4	10^{19}	1.11	−0.82	−0.30	0.88	−0.58	0.35
940314	164	13.8	10^{19}	0.51	−1.31	0.80	0.99	−1.71	0.07
940117	16	10.8	10^{19}	1.08	−0.94	−0.14	0.05	−0.40	0.44
940118	15	3.8	10^{17}	6.32	−5.95	−0.37	0.03	0.02	3.50
940119	15	2.0	10^{16}	9.55	−8.99	−0.56	−0.30	−0.08	3.23
940320	15	3.2	10^{16}	9.22	−8.05	−1.17	4.82	−0.68	4.47

near-pure normal or thrust fault mechanism (Table 2) which radiates Rayleigh-wave energy efficiently towards the north-eastern station cluster. Event 830124 has a larger non-double-couple component (CLVD) and is a combination of normal and strike-slip faulting at a centroid depth of 36 km. It has a complicated radiation pattern that varies considerably with frequency. The excitation amplitudes for this event are sensitive to changes in depth and average Earth structure in the source region. Owing to large phase gradients in the radiation pattern near the take-off azimuth, a small error in the moment tensor or take-off azimuth has a large influence on the observed phases at the stations. Refitting the waveforms after removing the strike-slip and CLVD components from the source mechanism provides path-averaged velocity models closer to the models for paths from the other events in the propagation corridor. Event 830124 has a magnitude some one point higher ($M_s = 6.6$) than the others in this cluster and it is likely that rupture effects have a larger influence on the seismograms from this event.

PROPAGATION CORRIDOR B

Propagation corridor B contains wave paths to eight stations from two events. For this corridor the mean and standard deviation of the relative amplitude anomalies were computed for each of the two events and are shown in Fig. 3. Fig. 3 shows that the anomalous amplitude spectra of the Rayleigh waves from one event do not lie within the standard deviation of the other event, indicating that the anomalies are related to the source rather than to along-path structure. The Californian stations lie in azimuths close to a node in the Rayleigh-wave radiation pattern for both these events, and hence the amplitudes are very sensitive to small errors in the moment tensor or take-off azimuth. To investigate this sensitivity, rotations of the moment tensor around a vertical axis were performed in a trial-and-error attempt to fit the two amplitude anomaly bands to each other. Rotation angles were limited from -20° to 20°, which is somewhat wider than the typical uncertainty range of $\pm 14^\circ$ (Helffrich 1997). Adopting the constraint that the path-averaged velocity models derived from the waveform fits based on the rotated moment tensors should remain similar, the rotations that moved the take-off azimuth through the radiation node could be rejected. With the same constraint a rotation moving the take-off azimuth away from the node of the moment tensor for 940314 could also be rejected. From the remaining possibilities, rotations from 0 to near -20° for the moment tensor of 930903, a rotation of -8° provides a substantial change in amplitude anomalies, so that the anomalies are, within standard deviations, equal to those of 940314 for periods over 40 s (Fig. 3b). However, the waveform fits deteriorate with increasing absolute rotation angle, while the path-averaged velocity models remain sufficiently similar for smaller angles but start to differ from those for 940314 near -20°. So a rotation of -8° in the moment tensor of 930903 in propagation corridor B can explain most of the amplitude discrepancy, but is not an entirely satisfactory explanation.

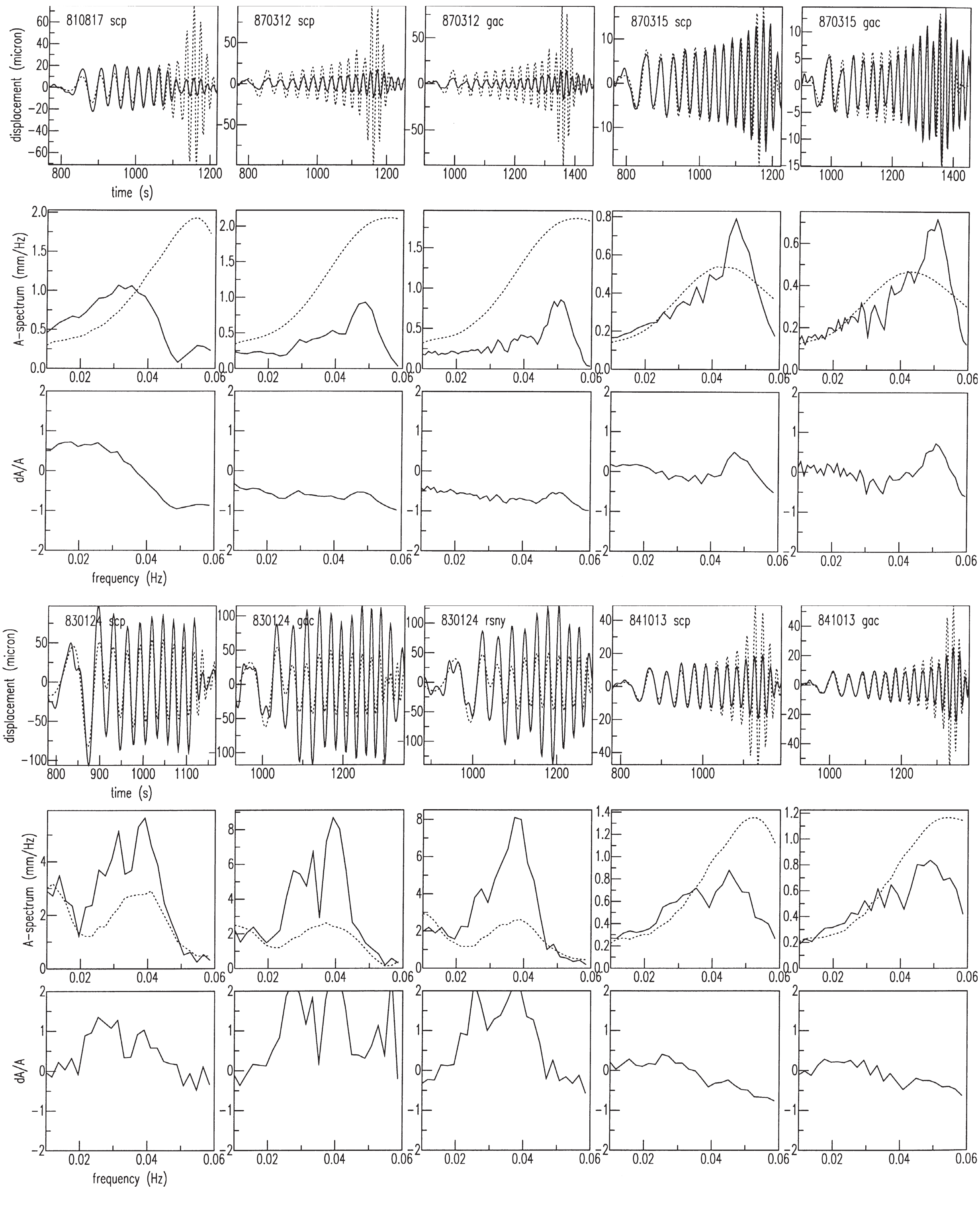

Figure 2. For propagation corridor A (Fig. 1): observed (solid) and predicted (dotted) vertical-component fundamental-mode Rayleigh waves (top), their amplitude spectra ('A-spectrum', where the solid and dotted lines correspond to the observed and predicted Rayleigh-wave amplitudes, respectively; centre) and the relative amplitude anomaly spectra dA/A (where $A = A_{\mathrm{predicted}}$ and $dA = A_{\mathrm{observed}} - A$; bottom). The displays are labelled by event ID and station name.

SOURCE DOMINATION OF AMPLITUDE ANOMALIES

Linear theories that are in principle suitable for amplitude inversions all relate the amplitude anomalies to relatively smooth far-field near-path structure (Woodhouse & Wong 1986; Snieder 1988a). Unfortunately, the data from propagation corridors A and B clearly show that the earthquake source seems to have, in different ways, a larger effect on amplitudes of intermediate-period fundamental-mode

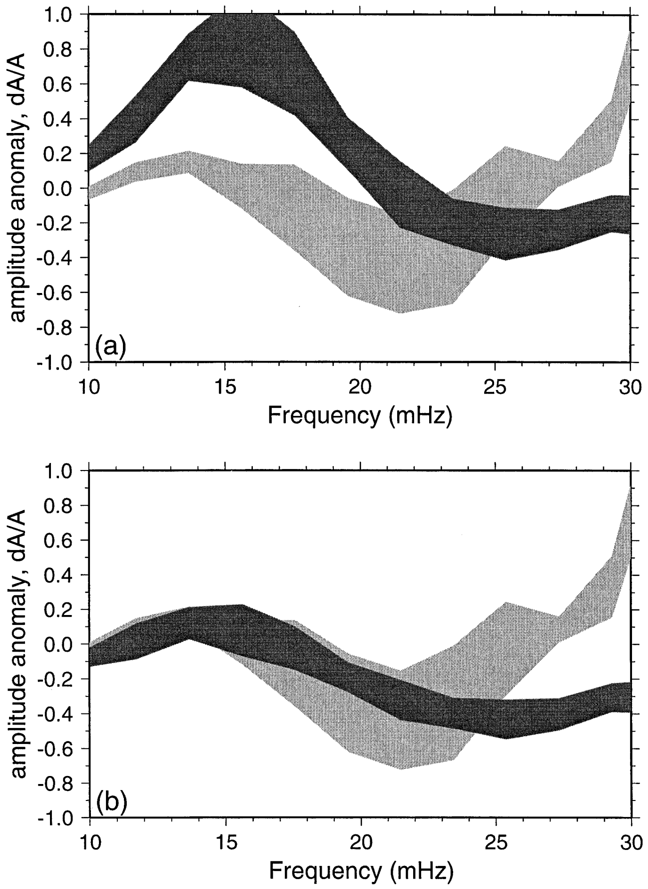

Figure 3. Relative amplitude anomaly spectra of fundamental-mode Rayleigh waves for propagation corridor B (Fig. 1). The grey bands are centred on their means and their width reflects twice the standard deviation of the relative amplitude anomalies of the Rayleigh waves from each of the two events within the corridor. (a) Bands computed for the catalogued CMTs. (b) Bands computed for MT 930903 rotated over $-8°$.

Rayleigh waves than variations in Earth structure along the path of wave propagation. One way in which the source affects Rayleigh-wave amplitude anomalies is through uncertainties in source parameters and Earth structure in the source region, as discussed above. This is not a unique explanation and the effects of such uncertainties are limited, as seen above. Therefore, an additional mechanism, which has a strong relation with the earthquake source, needs to be identified. Rayleigh-wave excitation amplitudes depend on the take-off azimuth from the source and the take-off azimuths of the recorded Rayleigh-wave energy depend on lateral heterogeneity. Um & Dahlen (1992) and Wang & Dahlen (1994) have shown that a mere perturbation, due to smooth heterogeneity, in the standard great-circle ray path (and hence also in its take-off azimuth) predicts amplitude anomalies that, in contrast to phase and arrival azimuth anomalies, do *not* match well with predictions from more accurate mode-coupling computations. The interaction between radiated Rayleigh-wave energy and heterogeneous structure is more complex than can be described by ray theory. Scattering could cause differences in the amplitude anomalies for different events if it was caused by structure of a roughness and size smaller than the Fresnel zones of the Rayleigh waves. This type of structure would have to be close enough to the source to produce similar anomalies at each station in one propagation corridor, as observed for corridors A and B. Heterogeneous structure is expected to be more abundant in seismically active regions than in stable continental regions, which predominantly house the observing seismic stations. However, such a biased distribution of heterogeneity alone does not explain all our observations since amplitude anomalies do not vary with station in propagation corridor B, while the dense station network lies in a seismically active region. We shall also see that the amplitude anomalies do vary among events in propagation corridor C, which lie in the same region as the stations of corridor B. Therefore, the dominant mechanism explaining the observed amplitude anomalies in fundamental-mode Rayleigh waves must be a combination of the earthquake source parameters and near-source structure.

SENSITIVITY KERNELS

Three-dimensional fundamental-mode Rayleigh-wave sensitivity kernels presented by Marquering, Nolet & Dahlen (1998) show that near-source and near-receiver structure in the Fresnel zone are very strong generators of scattered energy. To obtain this source–receiver symmetry in their sensitivity kernels, Marquering *et al.* (1998) neglect the interaction of the source mechanism with the sensitivity kernel. Meier *et al.* (1997) do take the source mechanism into account in their calculations, and their sensitivity kernel for the Rayleigh-wave amplitude of an event in the Philippine Sea shows that the sensitivity is strongest near the source. Following Meier *et al.* (1997), 20 mHz Rayleigh-wave amplitude sensitivity kernels for a station at 30° distance have been computed for all events discussed in this study (Fig. 4). The size of these amplitude sensitivity kernels is limited by the Fresnel zone approximation of Wang & Dahlen (1995). The computation of these sensitivity kernels takes the full source term **E**:**M**, as given by Dahlen (1979), into account. For simplicity, only forward Rayleigh-to-Rayleigh scattering of the form $\cos(\psi)$, where ψ is the scattering angle, is used. This form is an *ad hoc* but not unreasonable approximation, based on figures in Snieder (1988a). The exact scattering coefficients do not play an important role in this particular study. The geometric factor $[\sin(\Delta_1)\ \sin(\Delta_2)]^{-1/2}$, where Δ_1 and Δ_2 are the source-to-scatterer and the scatterer-to-receiver distances, respectively, is symmetric and equally enhances the sensitivity near the source and near the receiver. To demonstrate the effect of the source radiation this geometric factor has not been implemented for Fig. 4. Moreover, this factor is based on the far-field approximation and is abandoned when the scatterer is located within a couple of degrees from the source or receiver (Marquering *et al.* 1998). Full expressions for Rayleigh-wave sensitivity kernels can be found in Meier *et al.* (1997) and Marquering *et al.* (1998).

The amplitude sensitivity kernels in Fig. 4 show considerable to strong concentration of sensitivity near the source. The computed sensitivity kernels thus confirm the observations in this study that Rayleigh-wave amplitudes are dominantly affected by the source and near-source structure. While it is not possible in this study to identify uniquely

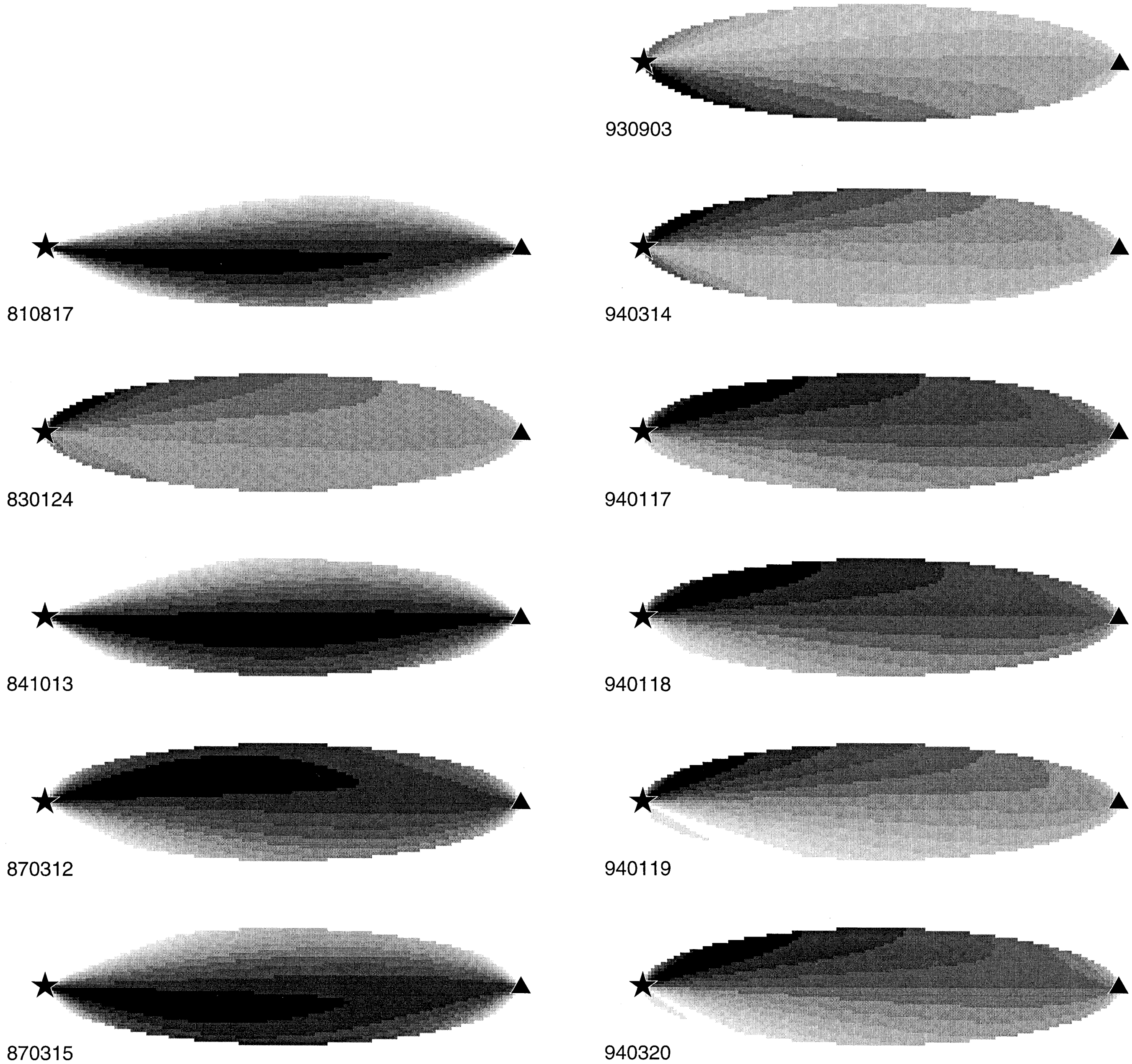

Figure 4. Grey-shade maps of the effect of the radiation pattern of an earthquake source (star) on the amplitude of Rayleigh waves scattered from points within the approximate first Fresnel zone. The representative station (triangle) is 30° from the source. The panels are labelled with the event ID and the source–receiver great circles have been rotated to run parallel in this figure. The grey shades are a linear function of the amplitude sensitivity, where black and white represent maximum and minimum sensitivity, respectively. The edge of the sensitivity kernels is determined with the Fresnel zone approximation of Wang and Dahlen (1995), which is based on phase coherency of the Rayleigh waves.

which particular parameters of the source and near-source structure are responsible for the observed amplitude anomalies, systematic inversion of amplitude anomalies for perturbations of source parameters and near-source structure should be the object of future work. It is interesting to note here that the postulated misrotation of the moment tensor of 930903 in propagation corridor B corresponds to a take-off azimuth of the Rayleigh waves that is 8° east of the great-circle azimuth. The sensitivity kernel is strongest at this perturbed azimuth from the source and it is likely that scattering of Rayleigh waves by the northwardly thickening continental crust plays a more important role than an actual misrotation of the moment tensor. The observations made in this study, together with the computed demonstration of dominant near-source sensitivity, strongly argue that near-field terms need to be incorporated in inverse scattering formulations before attempts to invert Rayleigh-wave amplitude anomalies can become successful.

PROPAGATION CORRIDOR C

Differences in near-source sensitivity, as demonstrated in Fig. 4, seem to play an important role in explaining the differences in the anomalous amplitude spectra within propagation corridors A and B. Propagation corridor C is a set of four wave paths from the 1994 January 17, $M_s = 6.8$ Northridge event (940117) and three aftershocks to station HRV of the Global Seismographic Network (GSN). Corridor C is different from corridors A and B in that the wave paths (Fig. 1) and amplitude sensitivity kernels (Fig. 4) are practically identical. The four events lie within less than half the wavelength of a 17 s Rayleigh wave from each other. Propagation corridor C thus provides the best circumstances for observing similar amplitude anomalies for the Rayleigh waves in the corridor. Indeed the waveforms of the Rayleigh waves from events 940117 and 940320, and hence also their relative amplitude anomalies, are practically identical (Fig. 5). On the other hand, the amplitude anomalies for events 940118 and 940119 are very different (Fig. 5). It should be noted that it is nearly impossible that such large differences, which are highly frequency-dependent and occur within hours, are related to changes in the HRV site or instrument response. Since Earth structure (at the source, near the source and along the path) is expected to have similar effects on the amplitudes for propagation corridor C, uncertainties in the source parameters are likely to play an important role in explaining these differences.

NORTHRIDGE SOURCE MECHANISM

The Northridge event (940117) featured slip on a buried thrust fault (e.g. Wald & Heaton 1994). The three aftershocks also mainly represent thrust faulting and seem to be located on the same thrust fault (Wald & Heaton 1994), which explains the similarities between the sensitivity kernels for propagation corridor C (Fig. 4). Pure thrust or normal events, as well as pure strike-slip events, excite fundamental-mode Rayleigh waves for all azimuths that have a pronounced spectral gap in the frequency band studied here (17–100 s) when the events occur between 5 and 50 km deep (for thrust/normal events) or between 11 and 70 km (for strike-slip events). This gap in the computed spectrum is what causes, for events 940118 and 940119, the large peaks near 30 mHz in the amplitude anomalies, and is the reason that, in the time domain, the Rayleigh waves look modulated (Fig. 5). This gap becomes a smooth spectral minimum for events 940117 and 940320 because these have a small but significant strike-slip component added to the thrust mechanism. Clearly the amplitude anomalies are very sensitive to such spectral gaps; a slight adjustment in the source mechanism can change the spectrum considerably. When, as an experiment, the centroid moment tensor found for the Northridge event (940117) is adopted for events 940118 and 940119, it puts their amplitude anomalies in line with those of 940117 and 940320 (Fig. 6). This is an encouraging result and it suggests that amplitude anomalies do not only carry information about near-source structure but can also be used to infer details in the source mechanism. In this case the amplitude anomalies seem to indicate that the slip on the thrust fault included a small right-lateral component. In explaining the presence of a spectral minimum rather than a spectral gap we cannot completely exclude near-source scattering. The frequency of a spectral gap resulting from pure thrust faulting depends on take-off azimuth. It is hence possible that two interfering waves with slightly different take-off azimuths undo each other's spectral gap in the observed record. Similarly, destructively interfering scattered waves can create

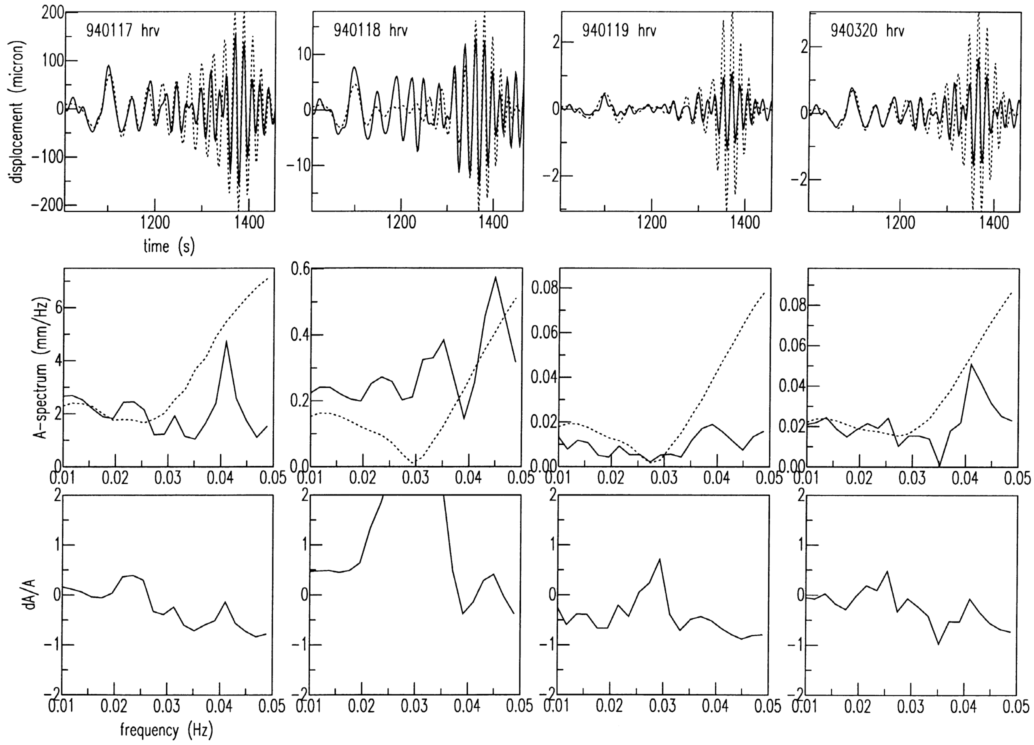

Figure 5. As Fig. 2, for propagation corridor C (Fig. 1).

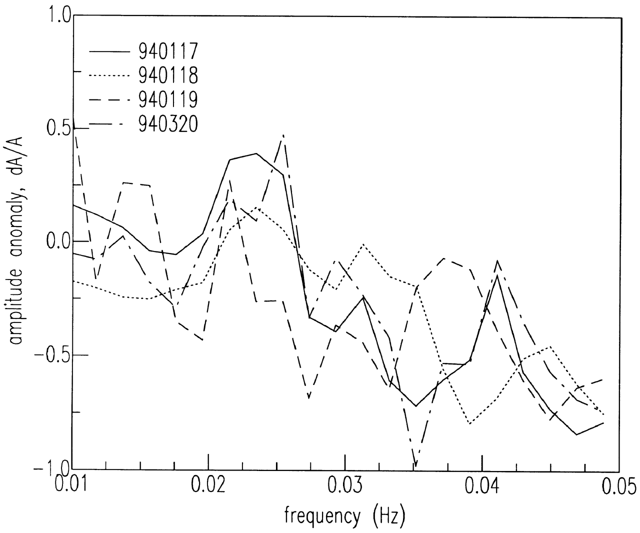

Figure 6. Relative amplitude anomaly spectra for the four events in propagation corridor C, after adopting the Northridge source mechanism for events 940118 and 940119.

a new gap or minimum. Spectral gaps picked in 44 teleseismic observations over a wide azimuth range of Rayleigh waves from the Northridge event suggest that although a pure thrust (rake $=90^\circ$) cannot be excluded for this event, it is less probable than the centroid rake of 110°, even when local average Earth structure and rupture propagation are taken into account (Van der Lee & Nolet 1997a). This agrees roughly with the average direction of rupture propagation during the Northridge event found by Wald & Heaton (1994). They used a preferred rake of 109° but could also not exclude a 90° rake, on the basis of their near-source strong-motion velocity waveform fits. It remains unclear why the reported centroid source parameters include lateral slip for the Northridge event but not for aftershocks on the same fault.

CONCLUSIONS

Amplitudes of intermediate-period fundamental-mode Rayleigh waves are very important constraints in determinations of earthquake source parameters. Amplitude anomalies that remain after taking the source parameters into account can be explained by various factors that are related to the source, the propagation path or the receiver. This paper shows that observed amplitude anomaly patterns of intermediate-frequency fundamental-mode Rayleigh waves are not related to receiver effects and are not, in contrast to phase anomalies, dominated by along- and near-path Earth structure, such as anomalous Q or heterogeneous velocity structure. Instead, we find that effects related to the earthquake sources dominate the anomalous amplitude spectra. These source effects range from uncertainties in the source parameters, through average Earth structure in the source region, to heterogeneous structure near the source. This implies that when such amplitude anomalies are inverted for along- and near-path elastic and anelastic structure, it is necessary to diminish source effects. Source effects can be minimized by using more than one station on a great-circle path or different great-circle orbits to the same station, as is common practice in global studies (Romanowicz 1994; Laske & Masters 1996). This, however, does not completely eliminate source effects since the sensitivity to heterogeneous structure, and hence also the computed take-off azimuth, is different for stations at different distances from the source along a great circle.

On the basis of this report of anomalous amplitude observations from only one take-off azimuth, we have not been able to distinguish the effects of uncertainties in the source parameters unambiguously from the effects of near-source scattering and we have found them exchangeable in various cases in this study. For example, it seems most probable that the contribution of a right-lateral slip component to the Northridge event and large aftershocks explains the amplitude anomaly discrepancies in propagation corridor C, but we cannot completely exclude near-source scattering. Rayleigh-wave sensitivity kernels that take the interaction with the radiation pattern into account show that the sensitivity of Rayleigh-wave amplitudes to heterogeneity is greatest near the source. Taking also into account that centroid source parameters are derived from a wide variety of seismic waves in a wide frequency band over a wide azimuth range, it seems most probable, for propagation corridors A and B, that near-source scattering dominates intermediate-period Rayleigh-wave amplitude anomalies. This report thus implies that it is necessary to incorporate near-field scattering, most importantly near the source, in amplitude anomaly inversion algorithms.

To separate source effects from path effects on the amplitude anomalies, we have identified, by trial and error, those source effects that are most likely to be responsible for the amplitude anomalies observed in this study. Correction for these source effects has optimized the consistency of the amplitude anomalies within each of the propagation corridors B and C (Figs 3b and 6). These results show that, under optimal conditions, the distribution of possibly path-related amplitude anomalies of Rayleigh waves in 30°-long propagation corridors has a standard deviation that ranges from 10 per cent to as much as 30 per cent. Under normal conditions this standard deviation easily exceeds 100 per cent (Figs 2, 3a and 5).

ACKNOWLEDGMENTS

Guust Nolet suggested the observation of Rayleigh-wave amplitudes and I thank him for many valuable comments regarding their interpretation. Discussions with Thomas Meier, Sergei Lebedev and Henk Marquering were very helpful and led me to compute the sensitivity kernels in Fig. 4. I also thank Guust Nolet and Selwyn Sacks for critically reading the manuscript, and Barbara Romanowicz, Erik Larson and Alan Beck for constructive comments. This work was supported by NSF grant EAR-9526372, Princeton University and the Carnegie Institution of Washington. The USGS-NEIC and the IRIS-DMC made the data available and the Harvard-CMT group made the centroid source parameters available. Figures were produced with SAC (Tapley & Tull 1991) and GMT (Wessel & Smith 1995).

REFERENCES

Alsina, D., Woodward, R.L. & Snieder, R.K., 1996. Shear wave velocity structure in North America from large-scale waveform inversions of surface waves, *J. geophys. Res.,* **101,** 15 969–15 986.

Dahlen, F.A., 1979. Exact and asymptotic synthetic multiplet spectra on an ellipsoidal earth, *Geophys. J. R. astr. Soc.,* **59,** 19–42.

Dziewonski, A.M., Chou, T.A. & Woodhouse, J.H., 1981. Determination of earthquake source parameters from waveform data for studies of global and regional seismicity. *J. geophys Res.,* **86,** 2825–2852.

Dziewonski, A.M., Ekström, G. & Salganik, M.P., 1992. Centroid-moment tensor solutions for July–September 1991, *Phys. Earth planet. Inter.,* **72,** 1–11.

Helffrich, G.R., 1997. How good are routinely determined focal mechanisms? Empirical statistics based on a comparison of Harvard, USGS and ERI moment tensors, *Geophys. J. Int.,* **131,** 741–750.

Laske, G. & Masters, G., 1996. Constraints on global phase velocity maps from long-period polarization data, *J. geophys. Res.,* **101,** 16 059–16 075.

Marquering, H., Nolet, G. & Dahlen, F.A., 1998. Three-dimensional waveform sensitivity kernels, *Geophys. J. Int.,* **132,** 521–534.

Meier, T., Lebedev, S., Nolet, G. & Dahlen, F.A., 1997. Diffraction tomography using multimode surface waves, *J. geophys. Res.,* **102,** 8255–8267.

Nolet, G., 1990. Partitioned waveform inversion and two-dimensional structure under the network of autonomously recording seismographs, *J. geophys. Res.,* **95,** 8499–8512.

Patton, H.J., 1998. Bias in the CMT moment for central Asian earthquakes: evidence from regional data, *J. geophys. Res.,* **in press.**

Romanowicz, B., 1994. On the measurement of anelastic attenuation using amplitudues of low frequency surface waves, *Phys. Earth planet. Inter.,* **84,** 179–191.

Romanowicz, B., 1995. A global tomographic model of shear attenuation in the upper mantle, *J. geophys. Res.,* **100,** 12 375–12 394.

Sipkin, S., 1986. Estimation of earthquake source parameters by the inversion of waveform data: global seismicity, 1981–1983, *Bull. seism. Soc. Am.,* **76,** 1515–1541.

Snieder, R., 1988a. Large-scale waveform inversions of surface waves for lateral heterogeneity 1. Theory and numerical examples, *J. geophys. Res.,* **93,** 12 055–12 065.

Snieder, R., 1988b. Large-scale waveform inversions of surface waves for lateral heterogeneity 2. Application to surface waves in Europe and the Mediterranean, *J. geophys. Res.,* **93,** 12 067–12 080.

Tapley, W.C. & Tull, J.E., 1991. *Guide to the Unix Version of SAC, Rev. 4, LLNL,* Regents of the University of California.

Um, J. & Dahlen, F.A., 1992. Source phase and amplitude anomalies of long-period surface waves, *Geophys. Res. Lett.,* **19,** 1575–1578.

Van der Lee, S., 1996. The earth's upper mantle: its structure beneath North America and the 660-km discontinuity beneath northern Europe, *PhD thesis,* Princeton University.

Van der Lee, S. & Nolet, G., 1997a. Observational evidence for source-dominated amplitude perturbations in Rayleigh waves from narrow ray bundles and from the Northridge event, *Suppl. EOS Trans., Am. geophys. Un.,* **78,** S213.

Van der Lee, S. & Nolet, G., 1997b. Upper mantle *S*-velocity structure of North America, *J. geophys. Res.,* **102,** 22 815–22 838.

Wald, D. J. & Heaton, T.H., 1994. A dislocation model of the 1994 Northridge, California, earthquake determined from strong ground motions, *USGS Open File Report,* **94–178.**

Wang, Z. & Dahlen, F.A., 1994. JWKB surface-wave seismograms on a laterally heterogeneous earth, *Geophys. J. Int.,* **119,** 381–401.

Wang, Z. & Dahlen, F.A., 1995. Validity of surface-wave ray theory on a laterally heterogeneous earth, *Geophys. J. Int.,* **123,** 757–773.

Wessel, P. & Smith, W.H.F., 1995. New version of the Generic Mapping Tools released, *EOS, Trans. Am. geophys. Un.,* **76,** 329.

Woodhouse, J.H. & Dziewonski, A.M., 1984. Mapping the upper mantle: three-dimensional modeling of earth structure by inversion of seismic waveforms, *J. geophys. Res.,* **89,** 5953–5986.

Woodhouse, J.H. & Wong, Y.K., 1986. Amplitude, phase and path anomalies of mantle waves, *Geophys. J. R. astr. Soc.,* **87,** 753–773.

Zhang, Y. & Tanimoto, T., 1993. High-resolution global upper mantle structure and plate tectonics, *J. geophys. Res.,* **98,** 9793–9823.

Zielhuis, A. & Nolet, G., 1994. Shear-wave velocity variations in the upper mantle beneath central Europe, *Geophys. J. Int.,* **117,** 695–715.

Zielhuis, A. & Van der Hilst, R.D., 1996. Upper-mantle shear velocity beneath eastern Australia from inversion of waveforms from SKIPPY portable arrays, *Geophys. J. Int.,* **127,** 1–16.